ARTICLE NO. 79-1663R

Effects of Spanwise Blowing on Two Fighter Airplane Configurations

Ernie L. Anglin* and Dale Satran†
NASA Langley Research Center, Hampton, Va.

NASA Langley Research Center has recently conducted an investigation to determine the effects of spanwise blowing on two configurations representative of current fighter airplanes. This research examined not only the longitudinal or performance effects but was especially oriented toward determining the lateral-directional effects, particularly in the stall/departure angle-of-attack range. The wind-tunnel tests included measurement of static and forced-oscillation aerodynamic data, visualization of the airflow changes over the wing created by the spanwise blowing, and free-flight model tests. Effects of blowing rate, chordwise location of the blowing ports, asymmetric blowing, and the effects of blowing on the effectiveness of conventional aerodynamic controls were investigated.

Nomenclature

The longitudinal forces and moments are referred to the wind-axis system and the lateral-directional data are referred to the body-axis system.

b = wing span, m (ft)
$\bar{c}$ = mean aerodynamic chord, m (ft)
C_D = drag coefficient, $F_D/\bar{q}S$
C_L = lift coefficient, $F_L/\bar{q}S$
$C_{L,0}$ = lift coefficient with spanwise blowing off
C_l = rolling moment coefficient, $M_x/\bar{q}Sb$
C_{l_p} = $\partial C_l/\partial(pb/2V)$
C_{l_β} = $\partial C_l/\partial\beta$
$C_{l_{\dot\beta}}$ = $\partial C_l/\partial\dot\beta$
C_m = pitching moment coefficient, $M_y/\bar{q}S\bar{c}$
$C_{m_{\delta h}}$ = horizontal tail pitch control effectiveness
C_n = yawing moment coefficient, $M_z/\bar{q}Sb$
$C_{n_p} = \dfrac{\partial C_n}{\partial(pb/2V)}$
$C_{n_r} = \dfrac{\partial C_n}{\partial(rb/2V)}$
$C_{n_\beta} = \dfrac{\partial C_n}{\partial\beta}$
$C_{n_{\dot\beta}} = \dfrac{\partial C_n}{\partial\dot\beta}$
C_T = thrust coefficient, $F_T/\bar{q}S$
f = frequency of oscillation, Hz
F_A = axial force, N (lb)
F_D = drag force, N (lb)
F_L = lift force, N (lb)
F_T = thrust for spanwise blowing, N (lb)
k = reduced frequency parameter, $\omega b/2V$
M_x = rolling moment, m-N (ft-lb)
M_y = pitching moment, m-N (ft-lb)
M_z = yawing moment, m-N (ft-lb)
p = roll rate, rad/s
$\bar{q}$ = freestream dynamic pressure, N/m^2 (lb/ft^2)
S = wing area, m^2 (ft^2)
V = freestream velocity, m/s (ft/s)
α = angle of attack, deg
β = angle of sideslip, deg
δ_a = aileron deflection (per side), positive for left roll, deg
δ_h = horizontal tail deflection, positive for nose-down pitch, deg
δ_r = rudder deflection, positive for nose-left yaw, deg
ΔC_L = incremental lift coefficient (blowing on- blowing off)
ΔC_l = incremental rolling moment coefficient
ΔC_n = incremental yawing moment coefficient
Λ = sweep angle of wing leading edge
ω = angular frequency, $2\pi f$

Presented as Paper 79-1663 at the AIAA Atmospheric Flight Mechanics Conference, Boulder, Colo., Aug. 6-8, 1979; submitted Nov. 9, 1979; revision received Feb. 28, 1980.

Index categories: Aerodynamics; Handling Qualities, Stability and Control.

*Aerospace Technologist, Transonic Aerodynamics Branch, Subsonic-Transonic Aerodynamics Division.

†Aerospace Technologist, Dynamics Stability Branch, Flight Mechanics Division.

Introduction

In recent years the increasing emphasis on improving the maneuverability of high-performance fighter aircraft has stimulated the development of various concepts for producing additional lift at high angles of attack. One of these concepts, which has been the subject of considerable research, is the concept of spanwise blowing.[1-4] The airflow on thin, highly sweptback wings at moderate-to-high angles of attack is characterized by a leading-edge separation which forms a stable vortex over the wing and provides large vortex lift increments. However, for moderately swept wings of higher aspect ratios, vortex breakdown occurs at low angles of attack. Blowing a discrete jet spanwise over the upper surface of such a wing in a direction essentially parallel to the leading edge enhances the leading-edge vortex and delays vortex breakdown to higher angles of attack with a resultant substantial increase in lift.[1]

Most of the previous work on spanwise blowing has concentrated on the performance effects. However, the lift improvements due to spanwise blowing are most significant at moderate-to-high angles of attack, where many present fighter airplanes experience significant degradations in lateral-directional stability and control characteristics because of complex aerodynamic flow interactions. In view of the large effect of spanwise blowing on wing aerodynamics and the vortex flow rearward from the wing, it is conceivable that spanwise blowing may have substantial effects, either beneficial or detrimental, on the lateral-directional stability and control. Hence, the research effort reported herein was conducted to study the effects of spanwise blowing on the low-speed, high angle of attack, lateral-directional stability and control characteristics of two configurations represen-

tative of fighter aircraft. This research encompassed wind-tunnel static and forced-oscillation aerodynamic measurements and a visualization of airflow changes over the wing created by spanwise blowing. Effects of blowing rate, chordwise location of the blowing ports, asymmetric blowing, and the effects of blowing on the effectiveness of conventional aerodynamic controls were investigated. Also free-flight model tests were made to determine the effects of spanwise blowing on the high angle of attack flight characteristics of the models.

Apparatus and Tests

Two models representative of current fighter configurations were used in the investigation. A sketch of the configuration on which the tests were run is shown in Fig. 1. This twin-engine configuration has a wing with a leading-edge sweep of 34 deg. A delta wing with a leading-edge sweep of 60 deg and the same area as the swept wing was also tested on the model. Both wings were tested with no wing leading-edge or trailing-edge flap deflections. For each model, six blowing port locations (three on each side of the fuselage) were provided, although only one port on each side was used at a time. The ports exited parallel to the leading edge of the wing, as shown in Fig. 1. The front, middle, and rear ports were located longitudinally so that the distance from the junction of the wing leading edge and fuselage to the ports were 20, 30, and 40% of the mean aerodynamic chord, respectively (see Fig. 1). The ports were formed from 0.9525 cm (0.375 in.) i.d. steel tubing which exited flush with the fuselage 1.1684 cm (0.46 in.) above the upper surface of the wing.

Static Tests

The static force tests were performed in the Langley 3.67 m (12 ft) low-speed tunnel at a dynamic pressure of 192 N/m^2 (4 lb/ft^2). The compressed air for the blowing ports was supplied to the model via copper air lines from an external shielded "trombone" plumbing arrangement which minimized air-pressure tares. The trombone was clamped rigidly to the sting and the shield was placed over the trombone and air line without touching them. The air line, trombone, and shield were adjusted until the wind-on aerodynamic data with the air line connected, plugged, and pressurized matched the wind-on data with the air line not attached. A separate air line system was used for right and left sides of the model.

For the spanwise blowing tests, thrust coefficients of 0.04, 0.08, and 0.12 were used. The desired level of C_T was set by opening a motorized valve in each air line system to increase the blowing pressure until the desired axial force had been created on the balance; the axial force being related to the blowing thrust coefficient by the relation $F_A = C_T \bar{q} S \sin\Lambda$. The motorized valves for the left and right ports were adjusted independently to insure that the yawing moment and side force balance readings remained at zero. Once the proper pressures for the desired blowing rate were set, the balance readout system was rezeroed so the data acquired would show only the aerodynamic changes and would not include the thrust increment. For the asymmetric spanwise blowing tests, only the left port was used with the balance readout system once again rezeroed to avoid including direct thrust increments in the data.

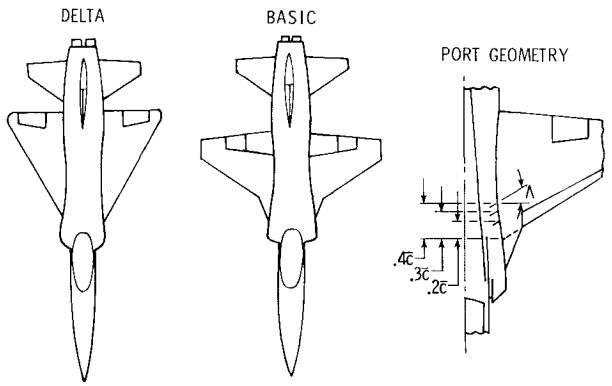

Fig. 1 Sketch of models and arrangement of spanwise blowing ports.

Forced-Oscillation Tests

The aerodynamic damping of the model was measured using a forced-oscillation method wherein the model is forced to oscillate about a given body axis at a fixed frequency and amplitude while the aerodynamic forces and moments are measured. A description of the forced-oscillation test equipment and data reduction procedures is given in Ref. 5.

The spanwise blowing forced-oscillation tests were made in the Langley 9.1 × 18.3 m (30 × 60 ft) tunnel at a dynamic pressure of 383 N/m^2 (8 lb/ft^2). Compressed air for the blowing ports was supplied through an air line, trombone, and shield system similar to that used in the static force tests. The air lines, trombone, and shield were again adjusted, as previously described, until they were not applying any static loads to the model. For the forced-oscillation tests, however, one further step was necessary so that the air line system did not affect the data. Wind-off tares for forced-oscillation tests are taken with the model, balance, and sting forced to oscillate about a given body axis at the same frequency and amplitude desired for the wind-on test condition. This procedure was used to remove the inertial effects of the model from the wind-on balance system readings so that the data acquired show only aerodynamic effects. Therefore, the air line system was adjusted until the wind-off forced-oscillation tares with the air line connected, plugged, and pressurized matched the tares with the air line disconnected.

Flow Visualization Tests

Flow visualization tests were performed during the static tests using a helium-bubble technique. A helium-bubble generator system formed streams of neutrally buoyant bubbles by blowing a helium-air mixture through a soap film inside a nozzle and then using a separate air line to blow the bubbles out of the nozzle, where tunnel airflow carried them downstream. With the tunnel lights off and the model painted black to reduce glare, the bubble streams were illuminated by a narrow beam of high-intensity light from a Xenon arc lamp. The bubbles traced the streamlines of the flow over the model and these flow patterns were recorded on a video tape system. Since the helium-bubble generating system produced better bubbles at lower speeds, the flow visualization tests were conducted at a dynamic pressure of 24 N/m^2 (0.5 lb/ft^2).

Free-Flight Tests

The dynamic stability and control characteristics of the basic model at angles of attack up to and including the stall/departure region were evaluated in the Langley full-scale tunnel using the free-flight model technique shown schematically in Fig. 2 and described in Ref. 6. In such tests, powered, instrumented, dynamically scaled models are flown by remote control in level flight through stall to investigate stability and control characteristics and to identify any tendencies of models to depart from controlled flight. Test results are typically in the form of pilot comments, movies, and time histories of flight-motion variables.

For the free-flight tests, engine thrust power is supplied by compressed air through plastic air hoses in an umbilical cable (see Ref. 6 for more detail). For the spanwise blowing free-flight tests, blowing air was supplied in a similar manner, with separate air lines for left and right ports. The spanwise blowing air supply lines were also completely independent of the engine thrust power line. The thrust level for the blowing ports was calibrated prior to the flight by mounting the model

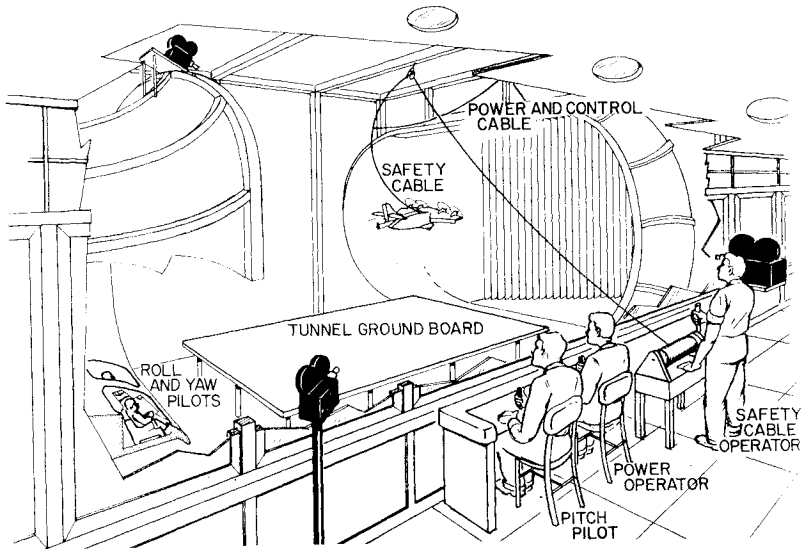

Fig. 2 Setup for free-flight tests.

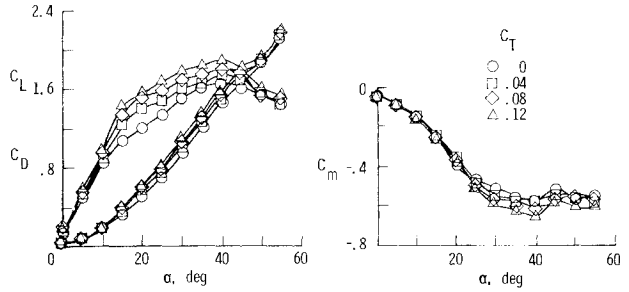

Fig. 3 Effect of spanwise blowing on the static longitudinal characteristics; basic configuration, $x/\bar{c} = 0.4$.

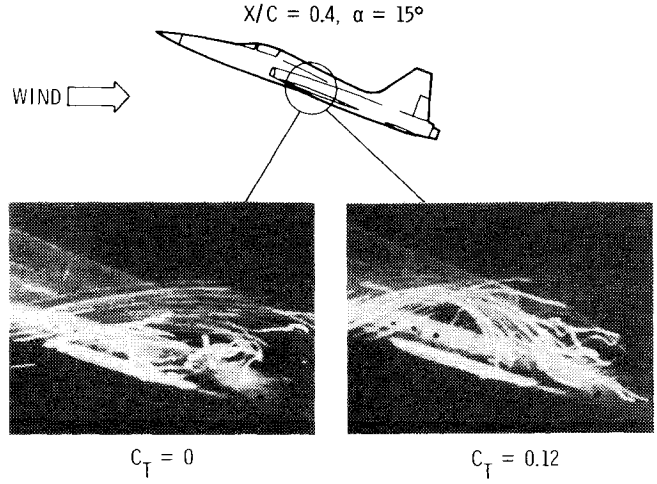

Fig. 4 Effect of spanwise blowing on the flow over the inboard section of the wing; basic configuration, $\alpha = 15$ deg, $x/\bar{c} = 0.4$.

to an external strain-gage balance. As it was impossible to change the blowing rate and keep the left and right ports balanced during the change without the strain-gage balance, the blowing rate was not changed during a flight. This caused the effective blowing C_T to increase during a flight as the dynamic pressure decreased when the flight progressed to higher angles of attack and thus higher lift coefficients. The preflight thrust could be set to give a desired C_T value only for a specific anglr of attack of interest for that particular flight. The free-flight tests were otherwise carried out using standard procedures.

Results and Discussion

Static Longitudinal Tests

The effects of spanwise blowing on the static longitudinal characteristics of the basic configuration are illustrated in Fig. 3 for three blowing rates from the rear port. As would be expected, the most obvious effect is that the lift coefficient was increased substantially as a result of the favorable spanwise flow gradients on the wing due to spanwise blowing, which enable the formation of a discrete wing leading-edge vortex originating at the breakpoint in the wing planform in addition to the enhancement of the existing vortex flow shed from the delta-shaped wing to fuselage fairing. This increase in lift is greatest in the 15-25 deg angle-of-attack range. Even the lowest blowing rate tested increased the lift coefficient at $\alpha = 15$ deg to a value that the configuration with no blowing did not achieve until $\alpha = 20$ deg. The maximum lift coefficient was increased from about 1.65 with no blowing to 1.9 for $C_T = 0.12$. However, the angle of attack for maximum lift remained unchanged by blowing. In the angle-of-attack range above 40 deg, the wing vortex breakdown occurs and the forebody vortex flowfield dominates,[7] and, as a result, spanwise blowing will have diminishing effects on the longitudinal characteristics. At an angle of attack of 0 deg the vortex flow should not be formed. The lift coefficient increase at 0 deg angle of attack with spanwise blowing is due to a jet-induced camber effect, as described in Ref. 3. The pitching moment curve shows that the static pitch stability was essentially unchanged at angles of attack up to 20 deg, and was increased somewhat in the 20 and 30 deg range.

The flow characteristics over the wing are illustrated in Fig. 4, where a side view of the inboard section of the wing at a 15 deg angle of attack is shown. With no spanwise blowing ($C_T = 0$), the flow over the wing shows separation and some reversed flow. With spanwise blowing ($C_T = 0.12$), the jet of air blown spanwise along the upper wing surface leads to the creation and/or enhancement of the vortex, thus causing the flow to be reattached to the wing.

The effects of spanwise blowing rates on the drag polar of the basic configuration are shown in Fig. 5. The drag polar indicates that spanwise blowing caused a marked reduction in drag for a given lift coefficient at moderate-to-high angles of attack. Inspection of Fig. 3 shows that in no case did spanwise blowing reduce drag at a given angle of attack, but that it permitted a given lift to be achieved at a lower angle of attack, and that at that angle of attack the drag was lower. This result is to be expected since, for wings with leading-edge separation

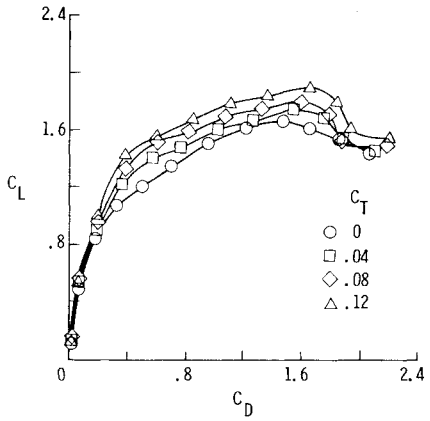

Fig. 5 Effect of spanwise blowing on the drag polar; basic configuration, $x/\bar{c}=0.4$.

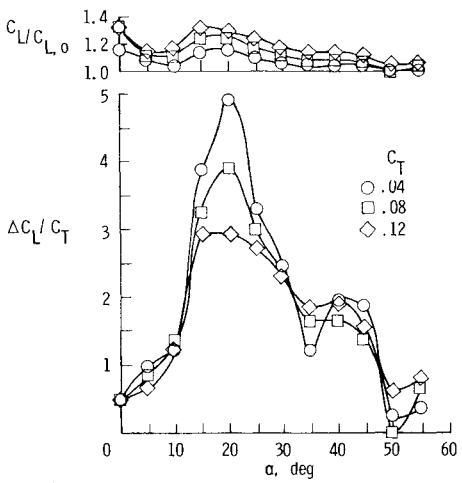

Fig. 6 Effect of spanwise blowing on the percentage lift increase and lift augmentation ratio; basic configuration, $x/\bar{c}=0.4$.

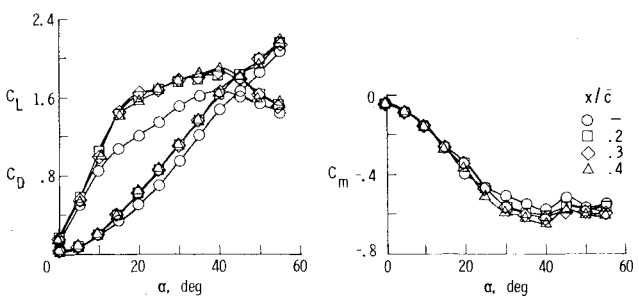

Fig. 7 Effect of longitudinal location of the spanwise blowing ports on the static longitudinal characteristics; basic configuration, $C_T=0.12$.

(including the case of leading-edge vortex flows), the drag due to lift varies as $C_L\tan\alpha$. There is an implication that such a reduction in drag automatically results in an improvement in performance. With a blowing system such as that represented herein, however, account must be taken of the loss of engine thrust from bleeding off the blowing air to determine whether there is a net gain in performance.

The efficiency of spanwise blowing for increasing the lift is shown in Fig. 6. The ratio of $C_L/C_{L,0}$ shows the greatest percentage increase in lift available with span blowing compared to no blowing is in the 15-20 deg angle-of-attack range, and gradually decreases at higher angles of attack. The lift augmentation ratio, $\Delta C_L/C_T$, indicates how efficiently spanwise blowing increases the lift of the wing compared to

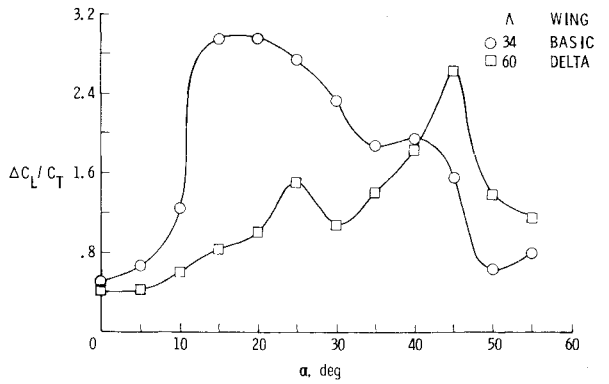

Fig. 8 Effect of spanwise blowing on the lift augmentation ratio; basic and delta wing configurations, $x/\bar{c}=0.4$ and $C_T=0.12$.

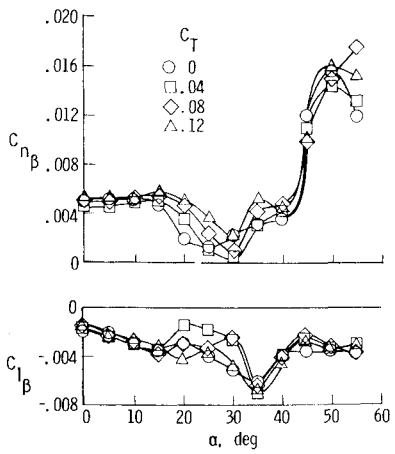

Fig. 9 Effect of spanwise blowing on the static lateral-directional stability; basic configuration, $x/\bar{c}=0.4$.

simply vectoring the blowing C_T in the direction of lift for thrust lift. The blowing effectiveness is greatest at 20 deg angle of attack, and spanwise blowing is more effective than vectored thrust in creating lift ($\Delta C_L/C_T>1.0$) from 10 deg up to about 45 deg angle of attack. The lift augmentation in the 15-30 deg angle-of-attack range is largest for the lowest blowing rate and decreases for the higher blowing rates. This indicates that the leading-edge vortex at the wing planform breakpoint is either created and/or stabilized by the lowest blowing rate and further increases in blowing rate causes only moderate enhancements of that vortex flow. In addition, the greatest benefit of spanwise blowing occurs at 20 deg angle of attack, where the wing without blowing has had a lift coefficient slope change due to the bursting of the vortex of the delta-shaped wing to fuselage fairing.

The effect of the longitudinal location of the blowing ports on the static longitudinal characteristics of the basic configuration is shown in Fig. 7 for $C_T=0.12$. These data show that port location had relatively little effect on longitudinal aerodynamics, which is consistent with the results obtained in Ref. 3.

Tests were also conducted with the model configured with the 60 deg delta wing to determine the effects of wing sweep on spanwise blowing characteristics. As expected, the effects of spanwise blowing on the longitudinal data for the delta wing were relatively small since a 60 deg delta wing already has a sizeable amount of natural vortex lift.[8] A comparison of the lift effectiveness for the basic and delta wing configurations is presented in Fig. 8. The substantial increase in lift augmentation ratio for the basic wing due to spanwise blowing occurred at a lower angle of attack than for the delta wing, because the leading-edge vortex breaks down at a lower angle of attack for lower sweep angles. Because the delta wing

already has a natural vortex flow, the lift effectiveness is less than 1.0 up to 20 deg angle of attack.

Static Lateral-Directional Stability

The effects of spanwise blowing on the static lateral-directional stability characteristics of the basic configuration are shown in Fig. 9 for the three blowing rates from the rear port. Blowing caused the directional stability derivative C_{n_β} to become more stable in the 15-25 deg angle-of-attack range. However, at 30 deg it caused C_{n_β} to become less stable. Spanwise blowing caused the effective dihedral C_{l_β} to decrease in the 15-30 deg angle-of-attack range, but to increase slightly at 35 deg angle of attack. The stall/departure for the basic configuration with no blowing has previously been observed to be at 30-35 deg angle of attack.[9] In this angle-of-attack range, no consistent effect of spanwise blowing exists on either C_{n_β} or C_{l_β}, so it appears from the static lateral-directional stability data that blowing would not be expected to have a significant effect on the stall/departure characteristics of this configuration because of any effect on directional stability or dihedral effect.

The flow characteristics over the wing and horizontal tail region are shown in Fig. 10 by a top view of the model at 25 deg angle of attack. With no spanwise blowing ($C_T = 0$), the flow rearward of the wing is random and appears to be separated over the horizontal tail. With blowing on ($C_T = 0.12$), the bubble stream shows organized and concentrated flow over the wing and rear fuselage and horizontal tail. This improved flow indicates that spanwise blowing delayed the reduction of dynamic pressure in the vertical tail region, which increases the vertical tail effectiveness and thus provides an explanation for the increased directional stability with spanwise blowing for this angle of attack shown in Fig. 9.

The effects of the longitudinal location of the spanwise blowing ports on the lateral-directional characteristics of the basic configuration are shown in Fig. 11. For all port locations tested, blowing improved C_{n_β} but had a detrimental effect on C_{l_β} in the 15-25 deg angle-of-attack range, with the rear port being obviously best for both C_{n_β} and C_{l_β}. In the 30-35 deg angle-of-attack range where stall/departure occurs, the rear port is also obviously best since the front and middle port locations had an unstable C_{n_β} value at $\alpha = 30$ deg. For all angles of attack, the rear port C_{n_β} was equal to or better than the C_{n_β} of the basic model with no blowing. The C_{l_β} data also show that significantly more stable values occurred in the divergence angle-of-attack range for the rear port location. It is important to note that the longitudinal location of the span blowing port has these significant effects on lateral-directional aerodynamics even though the longitudinal aerodynamic effects of port location were negligible (Fig. 7). It will be imperative, therefore, for any future proposed operational aircraft using spanwise blowing to have port location chosen with respect to optimizing the overall aerodynamic characteristics and not just the longitudinal characteristics.

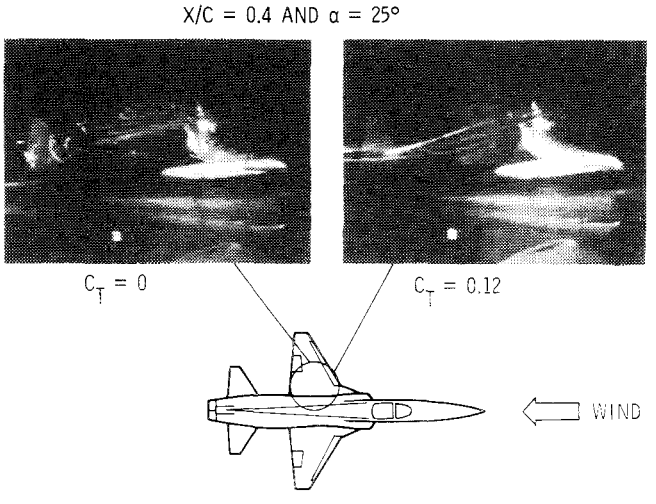

Fig. 10 Effect of spanwise blowing on the flow at the inboard section of the wing; basic configuration, $\alpha = 25$ deg and $x/\bar{c} = 0.4$.

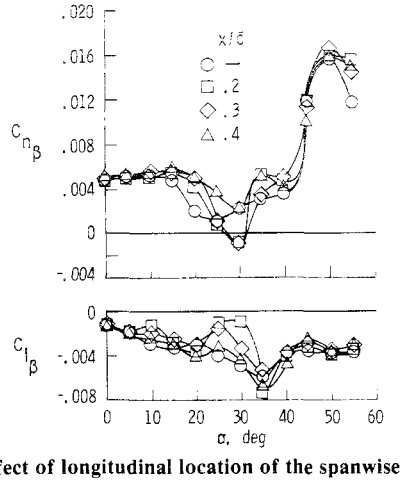

Fig. 11 Effect of longitudinal location of the spanwise blowing port on the static lateral-directional stability; basic configuration, $C_T = 0.12$.

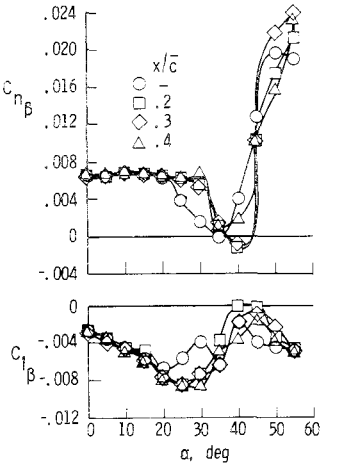

Fig. 12 Effect of longitudinal location of the spanwise blowing port on the static lateral-directional stability; delta wing configuration, $C_T = 0.08$.

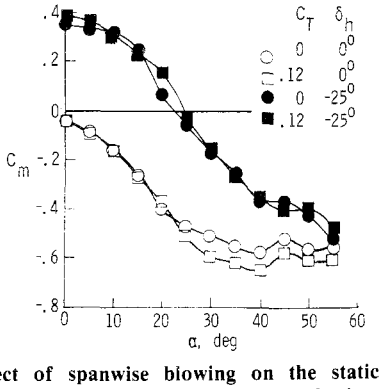

Fig. 13 Effect of spanwise blowing on the static longitudinal characteristics with horizontal tails deflected; basic configuration, $x/\bar{c} = 0.4$.

The effects of longitudinal blowing port location on the lateral-directional characteristics of the delta wing configuration are presented in Fig. 12. For the delta wing, spanwise blowing made both C_{n_β} and C_{l_β} more stable in the 20-35 deg angle-of-attack range. In addition, the delta wing showed that blowing effects on C_{n_β} were detrimental for all port locations tested from 35-45 deg angle of attack. In spite of the differences in trends for blowing effects for the basic and delta wing configurations, however, the rear port location again obviously was best for overall lateral-directional characteristics.

It should be specifically noted that the trends in the lateral-directional effects due to spanwise blowing were markedly different for the two configurations tested. This indicates that lateral-directional spanwise blowing effects are highly configuration-dependent.

Control Effectiveness

The effects of spanwise blowing on pitch control effectiveness for the basic configuration are presented in Fig. 13. These data show that blowing affects the magnitude of pitching moment for the controls neutral horizontal tail position for angles of attack higher than 25 deg, but that blowing has essentially no effect on the horizontal-tail-deflected data. What has probably occurred is that the more organized flow shown in the rear fuselage and horizontal tail area in Fig. 10 has made the horizontal tail more effective in the neutral position. Presenting the data of Fig. 13 in the form of a $C_{m_{\delta h}}$ vs angle-of-attack plot would indicate that spanwise blowing appreciably increased the magnitude of $C_{m_{\delta h}}$ above $\alpha = 25$ deg, but possibly would have led to the erroneous conclusion that those increased values of $C_{m_{\delta h}}$ meant that the use of blowing would allow a higher potential trim angle of attack to be achieved. The data of Fig. 13 do indicate that for $\delta_h = -25$ deg spanwise blowing increased trim angle of attack from about $\alpha = 23$ to 24.5 deg in an angle-of-attack range where the neutral horizontal tail data did not show any significant effect due to spanwise blowing.

The effect of spanwise blowing on the rudder effectiveness for the basic configuration is presented in Fig. 14. With a rudder deflection of -30 deg, the incremental yawing moment produced without blowing becomes negative at an angle of attack of 32 deg. Spanwise blowing increases the magnitude of incremental yawing moment and delays the negative values to significantly higher angles of attack. This improvement in rudder effectiveness with spanwise blowing is also attributed to the improved flow at the rear of the fuselage shown in Fig. 10.

The effects of spanwise blowing on aileron effectiveness are shown in Fig. 15. Spanwise blowing increased the incremental rolling moments up to 30 deg angle of attack. The relatively large improvement in aileron effectiveness due to blowing in the 10-20 deg angle-of-attack range may be attributed to the large improvements in flow (i.e., reattachment of the flow) on the rear portion of the wing due to spanwise blowing indicated in Fig. 4. With blowing, the ailerons produced a small adverse yawing moment which the model did not exhibit without blowing.

The effects of asymmetric spanwise blowing are shown in Fig. 16. Using asymmetric blowing for roll control would significantly increase the roll control available from 10-40 deg angle of attack. In this angle-of-attack range, the roll control provided by asymmetric blowing alone is comparable to the roll control provided by the ailerons at zero angle of attack. The disadvantage is that asymmetric spanwise blowing produces large adverse yawing moments at these angles of attack. Since the data presented include only the aerodynamic effects for the asymmetric spanwise blowing, the thrust effects on yawing moment should also be taken into account. However, an asymmetric thrust coefficient of 0.12 produces a positive yawing moment of only 0.0075, which is considerably smaller than the adverse aerodynamic yawing moments produced. The rudder control effectiveness data shown in Fig. 14 indicate that very large rudder deflections ($\delta_r > 30$ deg) would be needed to balance out the adverse yawing moments of this magnitude.

Forced-Oscillation Tests

The effect of spanwise blowing on the dynamic lateral-directional stability derivatives obtained during roll-oscillation tests is presented in Fig. 17. At 30-35 deg angle of attack where the directional divergence occurs, the roll-damping derivative $C_{l_p} + C_{l_\beta}\sin\alpha$ becomes highly positive

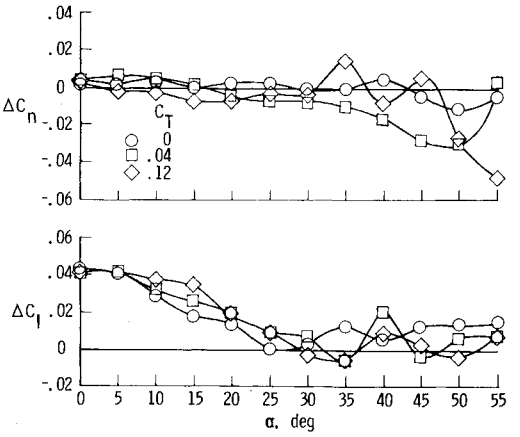

Fig. 15 Effect of spanwise blowing on the aileron effectiveness; basic configuration, $x/\bar{c} = 0.4$ and $\delta_a = -30$ deg.

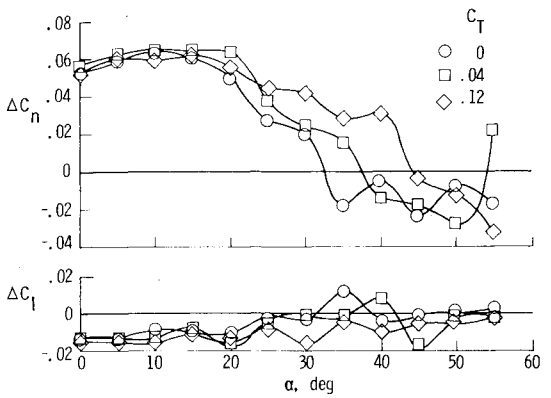

Fig. 14 Effect of spanwise blowing on the rudder effectiveness; basic configuration, $x/\bar{c} = 0.4$ and $\delta_r = -30$ deg.

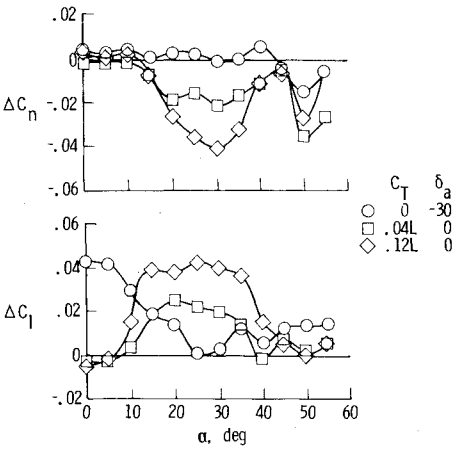

Fig. 16 Effect of asymmetric spanwise blowing on roll control; basic configuration, $x/\bar{c} = 0.4$.

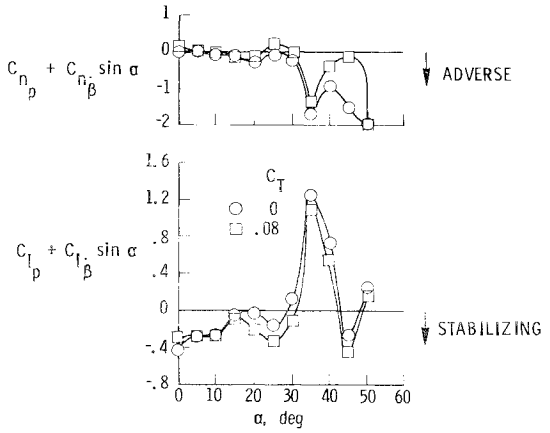

Fig. 17 Effect of spanwise blowing on the dynamic lateral-directional stability derivatives obtained during rolling oscillation tests; basic configuration, $x/\bar{c} = 0.4$, $k = 0.08$, and amplitude = ±5 deg.

(destabilizing) and the cross derivative $C_{n_p} + C_{n_{\dot\beta}} \sin\alpha$ becomes highly negative (adverse). The effect of spanwise blowing on both of these derivatives was in a beneficial direction, but the magnitude of the improvements was so small that blowing effects on the forced-oscillation roll derivatives would appear to have no significant effect on the directional divergence. The most significant effect due to spanwise blowing is the relatively large stable increase in $C_{l_p} + C_{l_{\dot\beta}} \sin\alpha$, together with a less adverse $C_{n_p} + C_{n_{\dot\beta}} \sin\alpha$ that occurs around 20 deg angle of attack.

Free-Flight Tests

In the free-flight tests of the basic configuration, spanwise blowing did not noticeably affect the longitudinal stability and control of the model, which was considered generally adequate for the angle-of-attack range tested. With blowing, the model could be flown to higher lift coefficients due to the creation and/or enhancement of vortex lift.

The stall/departure motion for this configuration is an apparent directional divergence associated with large unstable values of $C_{n_r} - C_{n_{\dot\beta}} \cos\alpha$ and $C_{l_p} + C_{l_{\dot\beta}} \sin\alpha$ coupled with lack of adequate control power in the 30-35 deg angle-of-attack range. (For a more detailed discussion of the stall/departure see Ref. 9 or 10.)

The maximum angle of attack (just above 30 deg) reached before the stall/departure occurred was not changed by use of spanwise blowing as was indicated by both the static data (Fig. 9) and the forced-oscillation data (Fig. 17). The departure motion was not apparently affected by the gains in rudder and/or aileron effectiveness due to spanwise blowing because these gains were relatively minor compared to the large unstable moments created by any yaw or roll motion in conjunction with the large unstable damping derivatives shown in Fig. 17. However, the pilot found the model to be easier to fly with spanwise blowing up to the divergence angle of attack due to the increased static and dynamic lateral-directional stability and rudder and aileron control power available at the lower angles of attack.

In the flight tests, the model without spanwise blowing and with roll and yaw dampers off exhibited a wing rock at 20 deg angle of attack. With either spanwise blowing or the use of roll and yaw dampers, the model had a much milder wing rock. With both blowing and roll and yaw dampers on the flights were smooth with no indication of wing rock. The improvement of the wing rock with spanwise blowing is probably due to the increased stability of the roll damping derivative at 20 deg angle of attack (Fig. 17).

Conclusions

The use of spanwise blowing created and/or enhanced vortex lift which increased the lift coefficient available at moderate-to-high angles of attack, and increased the maximum lift coefficient but did not affect the angle of attack at which maximum lift occurred. With blowing, the same lift coefficient could be achieved with a significantly lower level of drag, due primarily to the lower angle of attack at which that lift coefficient was obtained. Analysis of potential improvements in performance because of this drag reduction should include loss of engine thrust from bleeding off the blowing air which is not accounted for in the present data. Spanwise blowing produced no appreciable effect on longitudinal stability, and longitudinal position of the blowing port had no effect on the longitudinal aerodynamic characteristics. Spanwise blowing did significantly affect the static lateral-directional aerodynamics, even for conditions where longitudinal aerodynamics were not affected and the direction and magnitude of the lateral-directional effects were not only different over different portions of the angle-of-attack range, but were shown to vary with blowing rate and longitudinal location of the blowing ports and to be highly configuration-dependent. Blowing significantly increased both rudder and aileron control effectiveness and caused more stable roll damping. Use of asymmetric spanwise blowing could produce large roll control moments at moderate-to-high angles of attack, but would produce large adverse yawing moments that would require very large rudder deflections (over 30 deg) for coordinated control. In free-flight tests, use of spanwise blowing produced no change in the high angle of attack directional divergence of the basic configuration. Use of blowing helped eliminate a wing rock exhibited in the free-flight tests by the basic configuration at about 20 deg angle of attack.

References

[1] Bradley, R.G., Wray, W.D., and Smith, C.W., "An Experimental Investigation of Leading-Edge Vortex Augmentation by Blowing," NASA CR-132415, 1974.

[2] Dixon, C.J., "Lift and Control Augmentation by Spanwise Blowing Over Trailing Edge Flaps and Control Surfaces," Fourth Aircraft Design and Flight Test and Operations Meeting, Los Angeles, Calif., Aug. 1972.

[3] Campbell, J.F., "Effect of Spanwise Blowing on the Pressure Field and Vortex-Lift Characteristics of a 44° Swept Trapezoidal Wing," NASA TN D-7907, 1975.

[4] Cornish III, J.J. "High Lift Applications of Spanwise Blowing," ICAS Paper 70-09, Sept. 1970.

[5] Chambers, J.R., and Grafton, S.B., "Static and Dynamic Longitudinal Stability Derivatives of a Powered 1/9-Scale Model of a Tilt-Wing V/STOL Transport," NASA TN D-3591, 1966.

[6] Parlett, L.P. and Kirby, R.H., "Test Techniques Used by NASA for Investigating Dynamic Stability Characteristics of V/STOL Models," *Journal of Aircraft*, Vol. 1, Sept.-Oct. 1964, 260-266.

[7] Edwards, O.R., "Northrop F-5F Shark Nose Development," NASA CR-158936, 1978.

[8] Campbell, J.F., "Augmentation of Vortex Lift by Spanwise Blowing," *Journal of Aircraft*, Vol. 13, Sept. 1976, pp. 727-732.

[9] Grafton, S.B. and Chambers, J.R., "Wind-Tunnel Free-Flight Investigation of a Model of a Spin-Resistant Fighter Configuration," NASA TN D-7716, 1974.

[10] Satran, D.R., "The Effects of Spanwise Blowing on the Low-Speed Flight Characteristics of a Fighter Airplane Model," Master's Thesis, George Washington University, Dec. 1978.